

Local atomic configuration in mechanically synthesized Co-Fe-Ni alloys

Tomasz Pikula,
Dariusz Oleszak,
Jan K. Żurawicz,
Elżbieta Jartych

Abstract. Ternary Co-Fe-Ni alloys were prepared from the elemental powders by the mechanical alloying method. Structural properties and hyperfine interactions parameters were determined using X-ray diffraction and Mössbauer spectroscopy. X-ray diffraction proved that during milling Co-Fe-based solid solutions with b.c.c. lattice were formed in the case of $\text{Co}_{40}\text{Fe}_{40}\text{Ni}_{20}$ and $\text{Co}_{50}\text{Fe}_{40}\text{Ni}_{10}$ alloys, while for $\text{Co}_{52}\text{Fe}_{26}\text{Ni}_{22}$ and $\text{Co}_{65}\text{Fe}_{23}\text{Ni}_{12}$ compositions Co-Ni-based solid solutions with f.c.c. lattice were obtained. Mössbauer spectroscopy revealed similar values of the average hyperfine magnetic fields for all the alloys. These values corresponded to the different surroundings of ^{57}Fe isotopes by Co, Fe and Ni atoms, depending on the chemical composition of the alloy. The possible atomic configurations around ^{57}Fe isotopes were discussed on the basis of the local environment model under the assumption that only the first nearest neighbours contribute to the hyperfine magnetic field at ^{57}Fe site.

Key words: nanocrystalline alloys • mechanical alloying • hyperfine interactions • Mössbauer spectroscopy

Introduction

Mechanical alloying (MA) is a well-established method for producing a variety of materials, e.g.: crystalline, quasicrystalline, nanocrystalline, and amorphous materials. Mechanically synthesized Fe-based alloys have interesting magnetic properties, which suggest several applications.

In our previous work we proposed the mechanical alloying as the potential technology of production of bulk Co-Fe-Ni alloys with good soft magnetic properties. Such alloys reach the saturation magnetization of the order of 1.6–1.7 T and a relatively small coercive field. It allows to consider mechanically synthesized Co-Fe-Ni alloys as good soft magnetic materials [6]. Moreover, the coercive field of these alloys is a function of grain size and generally agrees with the random anisotropy model [3].

Besides interesting macroscopic magnetic properties, the mechanosynthesized Co-Fe-Ni alloys are characterized by the surprising hyperfine interactions. Namely, the average hyperfine magnetic fields have very similar values for all the investigated compositions. The aim of this work is an attempt to explain this effect on the basis of the local environment model.

Experimental details

Co, Fe and Ni powders with a purity of 99.9% were subjected to the mechanical alloying process in a Fritsch

T. Pikula, J. K. Żurawicz, E. Jartych ✉
Department of Experimental Physics,
Institute of Physics,
Technical University of Lublin,
38 Nadbystrzycka Str., 20-618 Lublin, Poland,
Tel.: +48 81 5384618, Fax: +48 81 5384671,
E-mail: e.jartych@pollub.pl

D. Oleszak
Faculty of Materials Science and Engineering,
Warsaw University of Technology,
141 Wołoska Str., 02-507 Warsaw, Poland

Received: 20 June 2006

Accepted: 11 November 2006

P5 planetary ball mill with a stainless-steel vial and balls. The initial dimensions of particles were 10 μm for Co, 6–9 μm for Fe and 3–7 μm for Ni. The compositions of alloys: $\text{Co}_{40}\text{Fe}_{40}\text{Ni}_{20}$, $\text{Co}_{50}\text{Fe}_{40}\text{Ni}_{10}$, $\text{Co}_{52}\text{Fe}_{26}\text{Ni}_{22}$ and $\text{Co}_{65}\text{Fe}_{23}\text{Ni}_{12}$ were chosen on the basis of the data reported in [8, 9]. All MA processes were performed under an argon atmosphere.

XRD measurements were carried out using a Philips PW 1830 diffractometer working in a continuous scanning mode with $\text{CuK}\alpha$ or $\text{CoK}\alpha$ radiation. The Williamson-Hall approach was used for determination of the average grain sizes, D , and the mean level of internal strains, ϵ , [11]. On the basis of the coherent polycrystal model [10], the volume fraction of the grain boundaries C_{gb} was determined by the formula

$$(1) \quad C_{gb} = 1 - f_g$$

where f_g denotes the volume fraction of the grains given by

$$(2) \quad f_g = (D - d)^3 / D^3$$

and d is the effective grain boundary thickness, which comprises 2–3 atomic layers, as suggested in Ref. [2].

MS studies were performed at room temperature in standard transmission geometry using a source of ^{57}Co in a rhodium matrix.

Results and discussion

XRD studies proved that alloys started to form after about 10 h of milling. Figure 1 shows the patterns obtained for the final products of milling (after 100 h). Detailed analysis of XRD results allowed to state that during MA process of $\text{Co}_{40}\text{Fe}_{40}\text{Ni}_{20}$ and $\text{Co}_{50}\text{Fe}_{40}\text{Ni}_{10}$ systems the solid solutions with b.c.c. (body-centred cubic) lattice were formed, while for $\text{Co}_{52}\text{Fe}_{26}\text{Ni}_{22}$ and $\text{Co}_{65}\text{Fe}_{23}\text{Ni}_{12}$ compositions solid solutions with f.c.c. (face-centred cubic) lattice were obtained. These results agree well with the phase-diagram for the bulk Co-rich Co-Fe-Ni alloys obtained by melting [7]. Moreover, the obtained alloys are disordered, e.g. Co, Fe and Ni atoms occupy the lattice sites randomly. Table 1 summarizes structural data for the final products of MA processes. The lattice parameters of the obtained alloys are similar to those reported for the electrodeposited binary Co-Fe (0.2848 nm for $\text{Co}_{60}\text{Fe}_{40}$ [5]) and Co-Ni (0.3513 nm for $\text{Co}_{55}\text{Ni}_{45}$ and 0.3531 nm for $\text{Co}_{65}\text{Ni}_{35}$ [4]) alloys. It may be supposed that in the mechanically synthesized $\text{Co}_{40}\text{Fe}_{40}\text{Ni}_{20}$ and $\text{Co}_{50}\text{Fe}_{40}\text{Ni}_{10}$ solid solutions the b.c.c.

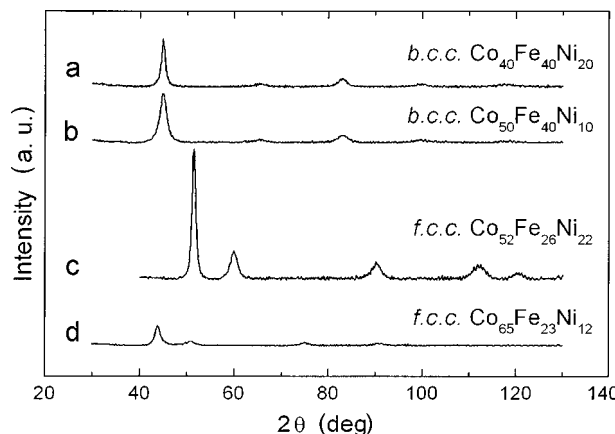


Fig. 1. XRD patterns of the mechanosynthesized Co-Fe-Ni alloys measured with $\text{CuK}\alpha$ (a), (b), (d) and $\text{CoK}\alpha$ (c) radiation.

Co-Fe alloy is the matrix, in which Ni atoms dissolve, while in the case of $\text{Co}_{52}\text{Fe}_{26}\text{Ni}_{22}$ and $\text{Co}_{65}\text{Fe}_{23}\text{Ni}_{12}$ solid solutions, the matrix is the f.c.c. Co-Ni alloy, in which Fe atoms dissolve.

It may be noticed (see Table 1) that in spite of the comparable conditions and the same starting materials, the obtained alloys have different grain sizes. This discrepancy may be due to the different chemical compositions of the alloys as well as the two other crystalline lattices. However, the values of the average grain sizes allow to consider all the alloys as nanocrystalline alloys (in all cases $D < 100$ nm).

Mössbauer spectroscopy allowed not only monitoring the process of the alloy formation, but also determining the local configuration of atoms in the nearest neighbourhood of ^{57}Fe isotopes. For all the investigated compositions, the spectra of the samples milled for 2 and 5 h were characteristic of α -iron. As milling time increased up to 10–20 h, the spectral lines were slightly broadened, i.e. the half-widths at half-maximum of the spectral lines were 0.15–0.17 $\text{mm}\cdot\text{s}^{-1}$. This broadening was the result of the alloy formation as well as the decrease of the grain sizes and a relatively high level of internal strains. In the course of further milling the process of interdiffusion of Co, Fe, and Ni atoms occurred and resulted in the final alloy. The Mössbauer spectra for the final products of MA processes are presented in Fig. 2. All the spectra were fitted using the hyperfine magnetic field, HMF, distribution as suggested by the relatively high values of the width of the spectral lines and disordered structure of the alloys. The linear correlation between HMF and isomer shift, IS, as well as between HMF and quadrupole splitting, QS, was assumed in the fitting procedure. The HMF

Table 1. Structural data for mechanically synthesized Co-Fe-Ni alloys; D – average grain sizes, ϵ – mean level of internal strains, C_{gb} – volume fraction of the grain boundaries, a – lattice parameter

Composition	Lattice	D (nm)	ϵ (%)	C_{gb} (%)	a (nm)
$\text{Co}_{40}\text{Fe}_{40}\text{Ni}_{20}$	b.c.c.	36(1)	1.20(5)	6(1)	0.2846(2)
$\text{Co}_{50}\text{Fe}_{40}\text{Ni}_{10}$	b.c.c.	15(1)	1.30(5)	14(1)	0.2843(4)
$\text{Co}_{52}\text{Fe}_{26}\text{Ni}_{22}$	f.c.c.	24(1)	0.72(5)	9(1)	0.3575(1)
$\text{Co}_{65}\text{Fe}_{23}\text{Ni}_{12}$	f.c.c.	10(1)	0.58(5)	21(1)	0.3581(10)

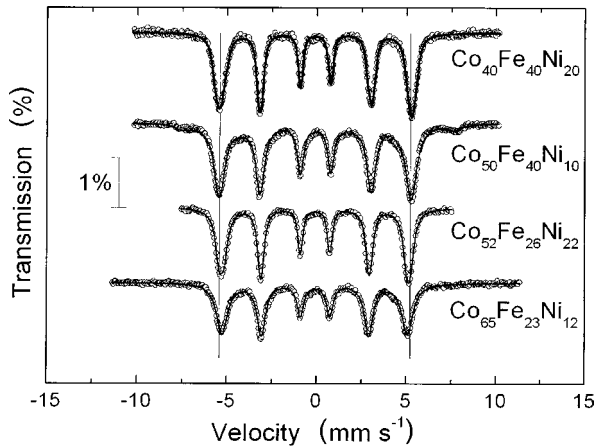


Fig. 2. Room-temperature Mössbauer spectra of the mechano-synthesized Co-Fe-Ni alloys; vertical lines denote the positions of spectral lines of α -iron.

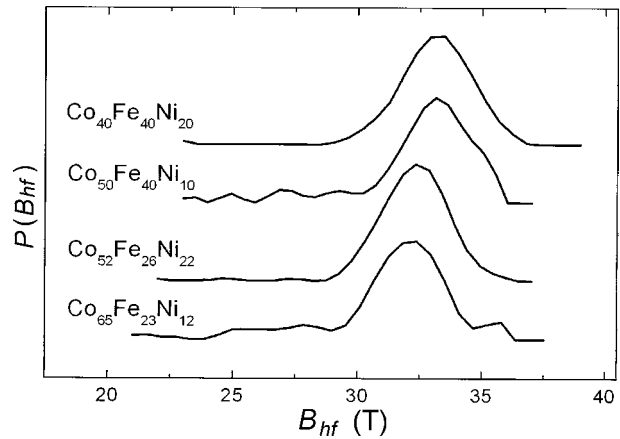


Fig. 3. Hyperfine magnetic field distributions for the mechano-synthesized Co-Fe-Ni alloys; $P(B_{hf})$ – probability in arbitrary units.

Table 2. Hyperfine magnetic fields and probable atomic configurations in mechanically synthesized Co-Fe-Ni alloys; $\langle B_{hf} \rangle$ – the average hyperfine magnetic field, B_{max} – the most probable HMF value

Composition	$\langle B_{hf} \rangle$ (T)	B_{max} (T)	(Co, Fe, Ni) configurations
Co ₄₀ Fe ₄₀ Ni ₂₀	33.09	33.48	(3, 3, 2) or (3, 4, 1) or (4, 3, 1)
Co ₅₀ Fe ₄₀ Ni ₁₀	32.17	33.13	(4, 3, 1) or (4, 4, 0) or (3, 5, 0)
Co ₅₂ Fe ₂₆ Ni ₂₂	32.24	32.34	(7, 3, 2) or (6, 3, 3)
Co ₆₅ Fe ₂₃ Ni ₁₂	31.21	32.37	(8, 3, 1) or (9, 2, 1)

values ranged from about 22 to 37 T (see Fig. 3). It may be noticed that all the HMF distributions are broad and the maximum of the curves for the b.c.c. alloys is slightly shifted towards higher values of HMF as compared to the f.c.c. alloys. The average values of the HMF obtained from the distributions are listed in Table 2 and their magnitude near 33 T may suggest the un-reacted α -iron contribution. However, XRD measurements exclude such a supposition.

The possible atomic configuration around ^{57}Fe isotopes was analysed under the assumption that only the first nearest neighbours (NN) contribute to the HMF at ^{57}Fe site. The probabilities of the various (Co, Fe, Ni) configurations in the NN shell were calculated using the generalized Bernoulli distribution [1]:

$$(3) \quad P_N(s, p, q) = \frac{N!}{s!p!q!} \cdot x^s \cdot y^p \cdot z^q$$

where N denotes the number of the first coordination sphere (8 for b.c.c. lattice and 12 for f.c.c. lattice), x, y, z – the chemical concentrations of the suitable component of the alloy and s, p, q – the number of the suitable atoms in the NN shell. The results of these calculations may be visualized by the diagram presented in Fig. 4. The most probable configurations are marked by the darkest grey colour, while those with insignificant probabilities are labelled by white colour. The maximum values of these probabilities obtained for the suitable (Co, Fe, Ni) configurations were attributed to the most probable HMF values, B_{max} , and they are listed in

Table 2. It may be noticed that not only one configuration of atoms in the NN shell of ^{57}Fe isotopes is possible in the mechanically synthesized Co-Fe-Ni alloys.

There are no papers concerning hyperfine interactions of the mechano-synthesized Co-Fe-Ni alloys in the modern literature to the authors' knowledge. The obtained values of the hyperfine magnetic fields may be compared with the data reported for the binary Co-Fe and Co-Ni alloys. As mentioned, the mechano-synthesized Co₄₀Fe₄₀Ni₂₀ and Co₅₀Fe₄₀Ni₁₀ alloys were b.c.c. solid solutions with the Co-Fe matrix in which Ni atoms were dissolved. The values of $\langle B_{hf} \rangle$ for Co₄₀Fe₆₀ and Co₅₀Fe₅₀ are about 35.6 and 34.9 T, respectively [5]. The magnitudes of $\langle B_{hf} \rangle$ for the Co₄₀Fe₄₀Ni₂₀ and

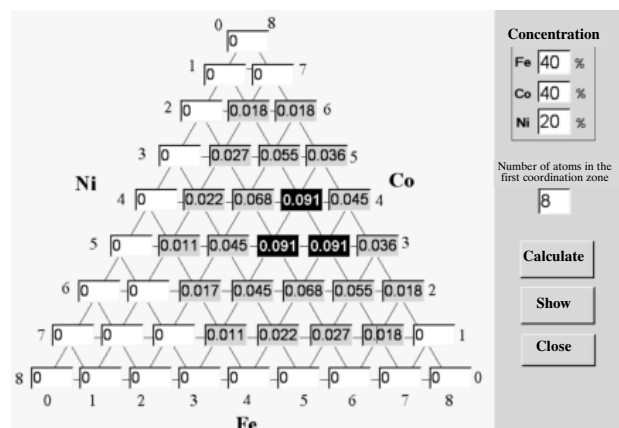


Fig. 4. An example of the configuration probability calculations for Co₄₀Fe₄₀Ni₂₀ alloy.

Co₅₀Fe₄₀Ni₁₀ alloys investigated in this work (i.e. 33.09 and 32.17 T) testify that Ni atoms significantly reduce the hyperfine magnetic field of these ternary alloys. On the other hand, in the case of Co₅₂Fe₂₆Ni₂₂ and Co₆₅Fe₂₃Ni₁₂ alloys, the f.c.c. solid solutions with the Co-Ni matrix were obtained during mechanosynthesis. The $\langle B_{hf} \rangle$ values for Co₅₀Ni₅₀ and Co₆₅Ni₃₅ are about 29.5 and 30.4 T, respectively [4]. It may be stated that iron atoms which dissolve in the Co-Ni matrix cause an increase of the effective hyperfine magnetic field of the ternary Co₅₂Fe₂₆Ni₂₂ and Co₆₅Fe₂₃Ni₁₂ alloys (32.24 and 31.21 T, respectively).

Conclusions

XRD and Mössbauer spectroscopy studies proved that during MA process the nanocrystalline Co₄₀Fe₄₀Ni₂₀, Co₅₀Fe₄₀Ni₁₀, Co₅₂Fe₂₆Ni₂₂ and Co₆₅Fe₂₃Ni₁₂ alloys were formed. The obtained alloys were characterized by the broad HMF distributions from which very similar average values of the hyperfine field were determined for each alloy. However, these values corresponded to the various configurations of Co, Fe, and Ni atoms in the nearest neighbourhood of ⁵⁷Fe isotopes, which were deduced on the basis of the extended binomial distribution.

The values of $\langle B_{hf} \rangle$ for mechanosynthesized Co-Fe-Ni alloys well correlate with the effective magnetic moments of the alloys. This problem will be a subject of further investigations.

References

1. Gerstenkorn T, Śródka T (1974) *Kombinatoryka i rachunek prawdopodobieństwa*. PWN, Warszawa
2. Grenèche JM, Ślavska-Waniewska A (2000) About the interfacial zone in nanocrystalline alloys. *J Magn Magn Mater* 215/216:264–267
3. Herzer G (1992) Nanocrystalline soft magnetic materials. *J Magn Magn Mater* 112:258–262
4. Jartych E, Olchowik J, Żurawicz JK, Budzyński M (1993) A Mössbauer spectroscopy study of electrodeposited (Co_xNi_{1-x})_{1-y}Fe_y alloys with $0 \leq x \leq 1$ and $y \leq 0.01$. *J Phys-Condens Matter* 5:8921–8926
5. Jartych E, Żurawicz JK, Budzyński M (1993) A Mössbauer study of electrodeposited Fe_{1-x}Co_x alloys. *J Phys-Condens Matter* 5:927–934
6. Jartych E, Żurawicz JK, Oleszak D, Pękała M (2006) Hyperfine interactions, structure and magnetic properties of nanocrystalline Co-Fe-Ni alloys prepared by mechanical alloying. *Hyperfine Interact* 168:989–994
7. Jen SU, Chiang HP, Chung CM, Kao MN (2001) Magnetic properties of Co-Fe-Ni films. *J Magn Magn Mater* 236:312–319
8. Liu X, Zangari G, Shen L (2000) Electrodeposition of soft, high moment Co-Fe-Ni thin films. *J Appl Phys* 87:5410–5412
9. Osaka T (2000) Electrodeposition of highly functional thin films for magnetic recording devices of the next century. *Electrochim Acta* 45:3311–3321
10. Song HW, Guo SR, Hu ZQ (1999) A coherent polycrystal model for the inverse Hall-Petch relation in nanocrystalline materials. *Nanostruct Mater* 11:203–210
11. Williamson GK, Hall WH (1953) X-ray line broadening from filed aluminium and wolfram. *Acta Metall* 1:22–31